Astron. & Astrophys. 43, 1—12 (1975)

Diffusion of Cosmic Rays in Non-thermal Radio Sources

A. S. Wilson
Sterrewacht, Leiden

Received January 29, revised May 6, 1975

Summary. We investigate spherically-symmetric models of extended non-thermal radio sources in which relativistic particles are generated by a compact source (e.g. pulsar) in the centre ($r=0$) and then diffuse away, losing energy by various processes. The main aim is to calculate the density of relativistic electrons $N(E, r, t)$ taking account of diffusion coefficients D and energy loss rates $d\varepsilon/d\tau$ which may be functions of energy, position and time. In Section 2 a simple physical picture is applied to solve problems in which D and $d\varepsilon/d\tau$ are arbitrary functions of energy and time, but independent of position. Special cases of astrophysical interest are then considered, in particular losses to ionization, bremsstrahlung, synchrotron radiation, inverse Compton scattering and uniform adiabatic expansion. Section 3 treats energy and position dependent parameters, but, for simplicity, the problem is now restricted to steady-state solutions. $N(E, r)$ is obtained here by a formal solution of the diffusion-loss equation. Detailed computations of the synchrotron spectra as a function of radius are made for representative dependences of D and $d\varepsilon/d\tau$ on energy and position, and the form of the spectrum of the integrated emission is calculated. The integrated spectrum of the Crab Nebula from radio to X-rays may be explained in terms of continuous injection of relativistic electrons having a power-law energy spectrum ($n_s(E_0) \propto E_0^{-1.52}$) over the whole range of energies (10^8eV to 10^{14}eV) into a magnetic field which decreases as r^{-1}. A more detailed comparison of the structure of the nebula and other radio sources with the models will be presented elsewhere.

Key words: cosmic rays — diffusion — Crab Nebula

1. Introduction

Current ideas on the origin of relativistic particles in non-thermal radio sources suggest that they may be injected by a central, compact object (pulsar, galactic nucleus etc.) into a more extended region. The concept of sources injecting fast particles into a large volume also arises in the galactic theory of cosmic rays, in which the relativistic protons and electrons are envisaged to be generated by supernovae and then fill the galactic disk. In this latter work, it is commonly assumed that the motion of the particles is diffusive (Ginzburg and Syrovatskii, 1964) in order to account for the high degree of isotropy of cosmic rays observed at the earth and the smooth variation of intensity and spectrum of the galactic radio background. We think it natural, therefore, to apply diffusion theory to radio sources and it is with such an application that this paper is concerned. Diffusion-loss models of the Crab Nebula, for example (Gratton, 1972; Wilson, 1972), give quite a good account of the observations. However, these papers assumed, for simplicity, that the magnetic field is spatially uniform, the diffusion coefficient independent of energy and position and that only synchrotron losses are important. The purpose of the present paper is to develop solutions for more realistic situations.

In Section 2 we solve problems in which the diffusion coefficient D and the rate of energy loss $d\varepsilon/d\tau$ are arbitrary functions of energy and time. Some particular processes of astrophysical interest are then considered, including losses to ionization, bremsstrahlung, synchrotron radiation, inverse Compton scattering and uniform adiabatic expansion. Section 3 is concerned with steady-state models with D and $d\varepsilon/d\tau$ dependent on energy and position. In a future communication we plan to compare these latter models with the size and spectrum of the X-ray source in the Crab Nebula, so computations of the spectrum of the synchrotron emissivity as a function of radius (Section 3.3) as well as the integrated radiation (Section 3.4) are presented. The results are also discussed from a physical point of view.

2. Models with Diffusion Coefficient and Rate of Energy Loss Arbitrary Functions of Energy and Time, but Independent of Position

Throughout the paper we shall be mostly concerned with a point source of relativistic electrons at $r=0$, as extended or multiple sources may often be dealt

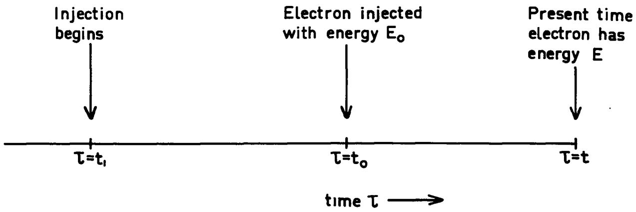

Fig. 1. Definition of time and energy parameters

with by appropriate integration of the point source solution. This section solves the problem of electrons being injected continuously, diffusing away from the source in an infinite, isotropic and homogeneous medium [diffusion coefficient $D(E, \tau)$] and losing energy by arbitrary processes [rate of energy loss $dE/d\tau(E, \tau)$]. The symbol E denotes the energy of an electron at the general time τ. The solution is then applied to some particular modes of energy loss of astrophysical interest.

To begin with, however, let us neglect the energy losses and imagine the source to create a burst of $n_s(E_0, t_0)dE_0dt_0$ electrons in the energy range $E=E_0$ to E_0+dE_0 between times $\tau=t_0$ and $t_0+dt_0(\tau=t_0$ represents the moment when the burst of particles under consideration was injected, $\tau=t$ the present time and, in cases of continuous injection, $\tau=t_1$ the instant when the particle source was switched on. $E=E_0$ denotes electron energy at injection and $E=E$ at the present time, see Fig. 1). At $\tau=t$ the number density of particles at distance r from the origin is given by the well-known expression (e.g. Morse and Feshbach, 1953):

$$dN(E_0, t_0, r, t)dE_0dt_0 = \frac{n_s(E_0, t_0)dE_0dt_0}{[4\pi \int_{t_0}^{t} D(E, \tau)d\tau]^{3/2}} \cdot \exp\left\{-\frac{r^2}{4\int_{t_0}^{t} D(E, \tau)d\tau}\right\}. \quad (1)$$

To incorporate the energy losses, let $f(E, E_0, t)$ represent the time taken for an electron to decay from energy E_0 to E, reaching E at t and let $E(E, E_0, t, \tau)$ be the energy of a particle at τ, the particle having been injected with E_0 at t_0 and reaching E at $t(t_0<\tau<t)$. The forms of f and E are governed by the nature of the energy losses under consideration and the time evolution of the radio source. t_0 may be eliminated from Eq. (1) by expressing it in terms of the other parameters (cf. Gratton, 1972):

$$t_0 = t - f(E, E_0, t).$$

Thus, writing $f'_E = \partial f/\partial E$

$$dN(E, E_0, r, t)dE_0dE = \frac{-n_s(E_0, t-f(E, E_0, t))dE_0 f'_E(E, E_0, t)dE}{\{4\pi \int_{t-f(E,E_0,t)}^{t} D[E(E, E_0, t, \tau), \tau]d\tau\}^{3/2}} \cdot \exp\left\{-\frac{r^2}{4\int_{t-f(E,E_0,t)}^{t} D[E(E, E_0, t, \tau), \tau]d\tau}\right\}. \quad (2)$$

Now imagine the spectrum $n_s(E_0, t_0)dE_0dt_0$ to be injected *continually* beginning at t_1. Some of the electrons which then comprise $N(E, r, t)$ were injected recently with an energy E_0 only a little greater than E, others longer ago with a higher energy, and so on. Thus the solution for continuous injection is simply

$$N(E, r, t)dE = -\int_{\mathrm{over}E_0} \frac{n_s(E_0, t-f(E, E_0, t))dE_0 f'_E(E, E_0, t)dE}{\{4\pi \int_{t-f(E,E_0,t)}^{t} D[E(E, E_0, t, \tau), \tau]d\tau\}^{3/2}} \cdot \exp\left\{-\frac{r^2}{4\int_{t-f(E,E_0,t)}^{t} D[E(E, E_0, t, \tau), \tau]d\tau}\right\}. \quad (3)$$

Equation (3) represents the general solution of the problem.

In astrophysical applications one is often concerned with

$$\left.\begin{aligned} n_s(E_0, t-f(E, E_0, t)) &= KE_0^{-\gamma}dE_0 \cdot E_0<E_* \\ &= O \qquad\quad E_0>E_* \end{aligned}\right\}. \quad (4)$$

The limits to the integral of Eq. (3) may then be evaluated as follows. The lower limit is obviously $E_0=E$, since only electrons with $E_0>E$ may contribute to $N(E, r, t)$. We identify 2 cases as far as the upper limit E_u is concerned.

Case a: $t-t_1<f(E, E_*, t)$.

This means that none of the electrons injected with the upper cut-off energy E_* have had time to decay to energy E at time t. All the electrons comprising $N(E, r, t)$ had an energy $E_0 \leqq E_u$ at injection (the equality is appropriate to electrons injected at t_1) such that

$$t-t_1 = f(E, E_u, t). \quad (5)$$

Hence E_u may be calculated when f and t_1 are known.

Case b: $t-t_1>f(E, E_*, t)$.

The upper limit to E_0 is now

$$E_u = E_*. \quad (6)$$

In the remainder of Section 2, Eq. (3) is evaluated for the source function of Eq. (4), some modes of energy loss of astrophysical interest and, for simplicity, a constant diffusion coefficient, D_0, independent of E and τ. Further work on energy dependent diffusion coefficients is presented in Section 3.

2.1. Rate of Energy Loss Time Independent $dE/d\tau = B(E)$

f is now independent of t and given by

$$f(E, E_0) = \int_{E_0}^{E} \frac{dE}{B(E)} > 0. \quad (7)$$

Equation (3) may be simplified by changing the variable of integration from E_0 to x where

$$x = \frac{r^2}{4D_0 f(E, E_0)}. \quad (8)$$

Letting

$$h(E, x) = \left(\frac{E}{E_0}\right)^{\gamma} f'_E$$

$$g(E, x) = f'_{E_0}$$

we find

$$\left.\begin{aligned} &N(E,r,t)=-\frac{KE^{-\gamma}}{4\pi D_0 r}\frac{1}{\sqrt{\pi}}\int_{x_l}^{\infty}\frac{h(E,x)}{g(E,x)}\frac{1}{\sqrt{x}}e^{-x}dx\\ &\text{where}\\ &\quad x_l=\frac{r^2}{4D_0(t-t_1)}\qquad \text{(Case a)}\\ &\quad x_l=\frac{r^2}{4D_0 f(E,E_*)}\qquad \text{(Case b)} \end{aligned}\right\}\tag{9}$$

2.1.1. $B(E)=-bE^q$ (b positive)

Thus

$$\left.\begin{aligned} f(E,E_0)&=(b(1-q))^{-1}[E_0^{1-q}-E^{1-q}]\quad \text{if}\quad q\neq 1\\ &=b^{-1}\ln(E_0/E)\quad \text{if}\quad q=1 \end{aligned}\right\}\tag{10}$$

i) $q\neq 1$

Equation (8) yields

$$N(E,r,t)=\frac{KE^{-\gamma}}{4\pi D_0 r}\frac{1}{\sqrt{\pi}}\int_{x_l}^{\infty}\left(1+\frac{r^2(1-q)b}{4D_0 x E^{1-q}}\right)^{-\left[\frac{\gamma-q}{1-q}\right]}\cdot\frac{1}{\sqrt{x}}e^{-x}dx\,.\tag{11}$$

Of interest is the case $E_*=\infty$. If $1-q>0$, case a [Eq. (5)] is then always obtained, since an electron of infinite energy takes an infinite time to decay to E and steady-state is never achieved. If, however, $1-q<0$ an electron of infinite energy decays to E in a finite time. A steady-state solution may thus be obtained after a sufficiently long time $(t-t_1>E^{1-q}/(q-1)b)$. x_l is then to be calculated from case b of Eq. (9), by substituting from Eq. (10) for $f(E,\infty)$:

$$x_l=-\frac{r^2(1-q)b}{4D_0 E^{1-q}}=\zeta\,.\tag{12}$$

We then use the relation

$$\begin{aligned}&\int_0^{\infty}(1+y)^{\left[\frac{\gamma-q}{1-q}\right]-1/2}y^{-\left[\frac{\gamma-q}{1-q}\right]}e^{-\zeta y}dy\\ &=\Gamma\left(\frac{1-\gamma}{1-q}\right)U\left(\frac{1-\gamma}{1-q},3/2,\zeta\right)\end{aligned}\tag{13}$$

which is valid when $\mathscr{R}\zeta>0$, $\mathscr{R}\left(\frac{1-\gamma}{1-q}\right)>0$ (Abramowitz and Stegun, 1965, p. 505). U is the confluent hypergeometric function of the second kind. Hence Eq. (11) becomes

$$N(E,r)=\frac{KE^{-\gamma}}{4\pi D_0 r}\frac{1}{\sqrt{\pi}}\zeta^{1/2}e^{-\zeta}\Gamma\left(\frac{1-\gamma}{1-q}\right)U\left(\frac{1-\gamma}{1-q},3/2,\zeta\right)\tag{14}$$

as long as $\gamma>1$. A special case of Eq. (14) (when $q=2$ i.e. losses appropriate to synchrotron radiation or inverse Compton scattering) has already been obtained by Webster (1970) and Gratton (1972).

ii) $q=1$

$$\left.\begin{aligned} &N(E,r,t)=\frac{KE^{-\gamma}}{4\pi D_0 r}\frac{1}{\sqrt{\pi}}\cdot\int_{x_l}^{\infty}\exp((1-\gamma)br^2/4D_0x)e^{-x}\frac{1}{\sqrt{x}}dx\\ &\text{with}\\ &\quad x_l=(r^2/4D_0(t-t_1))\qquad \text{(Case a)}\\ &\quad x_l=(br^2/4D_0\ln(E_*/E))\qquad \text{(Case b)} \end{aligned}\right\}\tag{15}$$

Note that here for case a the energy spectrum of the electrons $\propto E^{-\gamma}$ for all r, while for case b the effects of the upper cut-off are important.

2.1.2. Ionization, Bremsstrahlung, Synchrotron and Inverse Compton Losses Simultaneously

We neglect the slowly varying logarithmic term in the formula for the ionization losses (Ginzburg and Syrovatskii, 1964) and take

$$\frac{dE}{d\tau}=-k-lE-mE^2\,,$$

where the first term on the right-hand side represents the ionization losses, the second bremsstrahlung and the third losses to synchrotron radiation and inverse Compton scattering. See Ginzburg and Syrovatskii for the values of k, l, m. Thus

$$f(E,E_0)=\frac{2}{(4mk-l^2)^{1/2}}\cdot\left[\tan^{-1}\left(\frac{2mE_0+l}{(4mk-l^2)^{1/2}}\right)-\tan^{-1}\left(\frac{2mE+l}{(4mk-l^2)^{1/2}}\right)\right]$$

if $4mk>l^2$ (Case 1).
[Note that $0<\tan^{-1}(\quad)<\pi/2$ in this equation]
and

$$\begin{aligned}f(E,E_0)=(l^2-4mk)^{-1/2}&\left[\ln\left(\frac{2mE_0+l-(l^2-4mk)^{1/2}}{2mE_0+l+(l^2-4mk)^{1/2}}\right)\right.\\ &\left.-\ln\left(\frac{2mE+l-(l^2-4mk)^{1/2}}{2mE+l+(l^2-4mk)^{1/2}}\right)\right]\end{aligned}$$

if $4mk<l^2$ (Case 2).
Substitution in (9) yields, for both cases

$$N(E,r,t)=\frac{KE^{-\gamma}}{4\pi D_0 r}\frac{1}{\sqrt{\pi}}\int_{x_l}^{\infty}\left(\frac{E}{E_0}\right)^{\gamma}\left(\frac{k+lE_0+mE_0^2}{k+lE+mE^2}\right)\frac{1}{\sqrt{x}}e^{-x}dx.$$

The relation between E_0 and x may be readily found from Eq. (8), the value of x_l from Eq. (9) and we do not list these here.

2.2. *Rate of Energy Loss Dependent on Both Time and Energy*

As an illustrative example consider

$$\frac{dE}{d\tau}=-\frac{\alpha E}{\tau}-\frac{\beta E^2}{\tau^a}\,.\tag{16}$$

Equation (16) is of astrophysical interest since, when $\alpha=1$, it represents losses to uniform adiabatic expansion and synchrotron radiation simultaneously. τ is now to be measured from the explosion instant. If the expansion conserves magnetic flux ($H \propto \tau^{-2}$) then $a=4$, whereas if the field is maintained constant by some process $a=0$. By integrating (16) and taking particle energy E_0 at time $t-f(E, E_0, t)=t_0$ we find

$$E^{-1}t^{-\alpha}-E_0^{-1}(t-f)^{-\alpha}=(\beta/(a+\alpha-1)) \cdot [(t-f)^{1-a-\alpha}-t^{1-a-\alpha}]. \quad (17)$$

By substituting (17) in (3) the solution for the particle density becomes

$$N(E, r, t)=\frac{KE^{-\gamma}}{4\pi D_0 r}\frac{1}{\sqrt{\pi}}\int_{x_l}^{\infty}\left\{\left(1-\frac{u}{x}\right)^{\alpha} \cdot \left\{1-\frac{BEt^{1-a}}{(a+\alpha-1)}\left[\left(1-\frac{u}{x}\right)^{1-a-\alpha}-1\right]\right\}\right\}^{\gamma-2} \cdot \left(1-\frac{u}{x}\right)^{\alpha}\frac{1}{\sqrt{x}}e^{-x}dx, \quad (18)$$

where

$x=(r^2/4D_0 f(E, E_0, t))$

$u=(r^2/4D_0 t)$.

As before the two possibilities for x_l are:

Case a $\quad t-t_1<f(E, E_*, t)$

$\quad x_l=ut/(t-t_1)$.

Case b $\quad t-t_1>f(E, E_*, t)$

$\quad x_l=ut/f(E, E_*, t)$.

Note that if $E_*=\infty, f(E, E_*, t)$ may be written explicitly

$f(E, \infty, t)=t-[(a+\alpha-1)/(\beta Et^{\alpha})+t^{1-\alpha-a}]^{(1-\alpha-a)^{-1}}$.

3. Models with Diffusion Coefficient and Rate of Energy Loss Dependent on Energy and Position, But Not Time

Once the energy losses are a function of r, the method of Section 2 becomes more difficult to use, because a burst of particles which were monoenergetic at injection now have a spread of energies at any later time. The energy of any particular particle will depend on its past history and so even electrons at one particular radius will not be monoenergetic. Here we shall take the alternative approach of formally solving the differential equation of diffusion (cf. Syrovatskii, 1959; Webster, 1972). As before the relativistic electrons are generated by a point source at $r=0$. Since the diffusion coefficient and rate of energy loss are now time independent, E and τ may be abolished and replaced by E and t. Thus, we take

$$D(E, r)=D(E)r^n, \quad (19)$$

$$\frac{dE}{dt}(E, r)=B(E)r^m, \quad (20)$$

where $D(E)$ and $B(E)$ are arbitrary functions and, for the moment, n and m any real numbers (restrictions on the ranges of n and m are, however, introduced later). Such power-law dependences of D and dE/dt on r might, for example, result from pulsar models in which the pulsar governs the magnetic field strength and thermal gas density at a given distance from it (and hence the variation of synchrotron losses and, perhaps, diffusion coefficient with radius) as well as accelerating relativistic electrons in its immediate neighbourhood. In any case, radial dependences of this form seem sufficiently general for our purposes.

3.1. Solution of the Diffusion Loss Equation

For a monoenergetic injection spectrum (at energy E_0), the diffusion loss equation for our situation is

$$\frac{\partial N}{\partial t}-\text{div}[D(E, r)\text{grad}N]+\frac{\partial}{\partial E}\left[N\frac{dE}{dt}(E, r)\right] =\delta(r)\delta(E-E_0)K(E_0). \quad (21)$$

In the appendix, this equation is solved for $N(E, r)$ assuming D and dE/dt have the forms given by Eqs. (19) and (20) and that $\partial N/\partial t=0$ (steady-state). The boundary conditions are:

i) As $r\to\infty$, $N(E, r)\to 0$ and

ii) As $r\to 0$, $N(E, r)$ tends to the solution for *no* energy losses.

The solution is [Eq. (A9)]:

$$N(E, r)=\frac{(m-n+2)^{-2(n+1)/(m-n+2)}}{\Gamma((n+1)/(m-n+2))4\pi(n+1)}\frac{K(E_0)}{|B(E)|} \cdot \left|\int_{E_0}^{E}\frac{D(E)}{B(E)}dE\right|^{-(m+3)/(m-n+2)} \cdot \exp\left\{-\frac{r^{m-n+2}}{(m-n+2)^2\int_{E_0}^{E}(D(E)/B(E))dE}\right\} \quad (22)$$

subject to the conditions

$$m-n+2>0, \quad (23)$$

$$n+1>0. \quad (24)$$

The physical significance of Eqs. (23) and (24) is discussed later in Section 3.2.

To find $N(E, r)$ when the injection spectrum is a power law ($K(E_0)=KE_0^{-\gamma}$), Eq. (22) must be integrated over E_0 and this is done in the appendix for the case of

$$D(E)=D_0E^p, \quad (25)$$

$$B(E)=-bE^q, \quad (26)$$

where p and q are any real numbers and D_0 and b positive constants. The result for $N(E, r)$ [Eqs. (A15) and (A18)] depends on the sign of $p-q+1$:

i) $p-q+1<0$

$$N(E,r)=\frac{(m-n+2)^{-2(n+1)/(m-n+2)}K\Gamma((1-\gamma)/(p-q+1))}{4\pi(n+1)\Gamma((n+1)/(m-n+2))b(q-p-1)} \cdot \left|\frac{b(q-p-1)}{D_0}\right|^{(m+3)/(m-n+2)} \cdot E^{-\gamma+1-q-\frac{(p-q+1)(m+3)}{(m-n+2)}} \cdot \exp\left\{-\frac{b(q-p-1)r^{m-n+2}}{(m-n+2)^2 D_0 E^{p-q+1}}\right\} \cdot U\left(\frac{1-\gamma}{p-q+1}, 1+\frac{n+1}{m-n+2}, \frac{b(q-p-1)r^{m-n+2}}{(m-n+2)^2 D_0 E^{p-q+1}}\right). \quad (27)$$

ii) $p-q+1>0$

$$N(E,r) = \frac{(m-n+2)^{-2(n+1)/(m-n+2)}K\Gamma\left(\frac{p-q+\gamma}{p-q+1}+\frac{n+1}{m-n+2}\right)}{4\pi(n+1)\Gamma((n+1)/(m-n+2))b(p-q+1)} \cdot \left|\frac{b(p-q+1)}{D_0}\right|^{(m+3)/(m-n+2)} \cdot E^{-\gamma+1-q-\frac{(p-q+1)(m+3)}{(m-n+2)}} \cdot U\left(\frac{p-q+\gamma}{p-q+1}+\frac{n+1}{m-n+2}, 1+\frac{n+1}{m-n+2}, \frac{b(p-q+1)r^{m-n+2}}{(m-n+2)^2 D_0 E^{p-q+1}}\right), \quad (28)$$

where U is the confluent hypergeometric function of the second kind. Equations (27) and (28) are valid when $\gamma>1$ and when conditions (23) and (24) are satisfied. In the limiting cases of negligible and large energy losses, (27) and (28) assume simpler forms, which are also given in the appendix [Eqs. (A16), (A17) and (A19)].

3.2. Effect of the Singularity at the Origin and the Physical Significance of the Results

The reader will be aware that when n or m is negative the diffusion coefficient ($D\propto r^n$) or energy losses ($dE/dt\propto r^m$) become infinite at the origin. It is important to discuss the physical significance of our results in the presence of such singularities. In this subsection we demonstrate the reasons for restrictions (23) and (24) and that our solutions are physically meaningful when these conditions are met.

Consider the diffusion from the point source in the absence of energy losses and assume a steady-state exists. If the source generates n_s particles per second and $D=D_0 r^n$, the solution of the diffusion equation which has $N\to 0$ as $r\to\infty$ is

$$N(r)=\frac{n_s r^{-(n+1)}}{4\pi D_0(n+1)}, \quad (29)$$

when $n+1>0$.

Since the flux of particles crossing any sphere centred on the origin is n_s, we could envisage the electrons to be generated on the surface of a sphere of radius $r_0 (r_0<r)$ and find exactly the same solution for N. Thus, when we take account of the energy losses, we may imagine the electrons as produced at the surface of a small sphere surrounding the origin (and hence avoid any singularities) as long as the flux crossing the sphere at each energy is the same as that which left the point source i.e. *as long as the particles do not lose much energy in reaching* r_0. We have, in fact, automatically satisfied this condition by demanding that, as $r\to 0$, the solution tends to that for no energy losses. It may be readily shown that when $m-n+2\leq 0$, energy losses at the origin are catastrophic. This is the physical interpretation of Eq. (23). Problems with $m-n+2\leq 0$ may, of course, be approached by specifying the inner boundary condition at r_0 (cf. Webster and Longair, 1971); the solution for N is then a function of r_0 and we shall not consider such cases here.

To obtain insight into condition (24), $n+1>0$, we again neglect energy losses and begin with the solution for the particle density $dN(r,t)$ from a burst of $n_s dt_0$ particles injected between $\tau=t_0$ and t_0+dt_0 (see Fig. 1 for time definitions)

$$dN(r,t)=\frac{n_s dt_0}{B(t-t_0)^{3/(2-n)}}\exp\left\{-\frac{r^{2-n}}{D_0(2-n)^2(t-t_0)}\right\}.$$

To avoid divergence of the total number of particles as $r\to\infty$ we assume $2-n>0$ when

$$B=\frac{4\pi}{(2-n)}[D_0(2-n)^2]^{3/(2-n)}\Gamma\left(\frac{3}{2-n}\right).$$

The density resulting from steady injection from $\tau=t_1$ to $\tau=t$ is therefore,

$$N(r,t)=\int_{t_1}^{t}\frac{n_s dt_0}{B(t-t_0)^{3/(2-n)}}\exp\left\{-\frac{r^{2-n}}{D_0(2-n)^2(t-t_0)}\right\} = \frac{n_s}{B}\frac{[D_0(2-n)^2]^{(1+n)/(2-n)}}{r^{n+1}}\int_{u_1}^{\infty}u^{((1+n)/(2-n))-1}e^{-u}du,$$

where

$$u_1=\frac{r^{2-n}}{D_0(2-n)^2(t-t_1)}.$$

Thus

$$N(r,t)=\frac{n_s}{B}\frac{[D_0(2-n)^2]^{(1+n)/(2-n)}}{r^{n+1}} \cdot \Gamma\left(\frac{1+n}{2-n}, \frac{r^{2-n}}{D_0(2-n)^2(t-t_1)}\right),$$

where $\Gamma\left(\frac{1+n}{2-n}, \frac{r^{2-n}}{D_0(2-n)^2(t-t_1)}\right)$ is an incomplete gamma function. Now as $t\to\infty$, $u_1\to 0$ and if $(1+n)/(2-n)>0$ (i.e. $-1<n<2$) we have

$$N(r,t)=\frac{n_s r^{-(n+1)}}{4\pi D_0(n+1)}$$

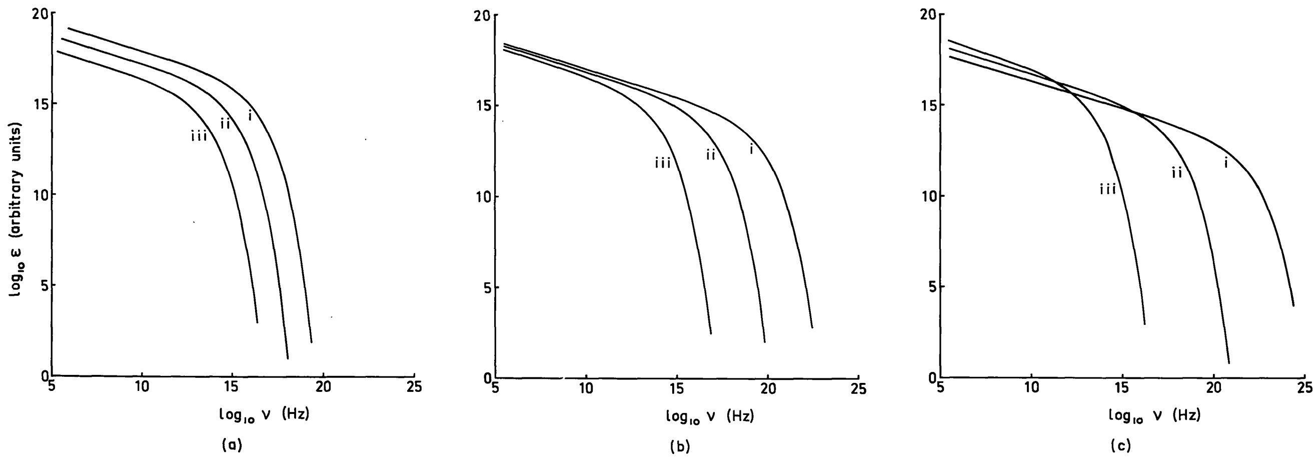

Fig. 2a—c. Illustrating the effect of changing m when $p=0$ and $n=-0.9$. (a) $m=-2$, (b) $m=0$, (c) $m=2$

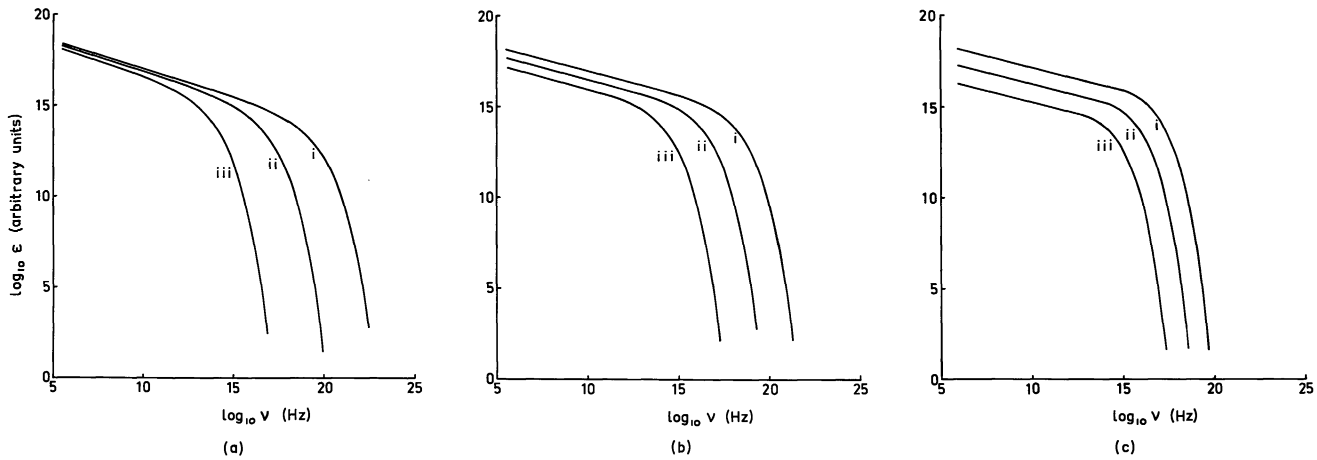

Fig. 3a—c. Illustrating the effect of changing n when $p=0$ and $m=0$. (a) $n=-0.9$, (b) $n=0$, (c) $n=0.9$

Figs. 2—5. Plots of $\log_{10}$ (synchrotron emissivity) vs $\log_{10}$ (frequency) from the models of Section 3. In each graph, three curves are drawn and marked *i*, *ii* and *iii*. Curve *i* is the spectrum at $r=10^{18}$ cm, Curve *ii* at $r=3\cdot 10^{18}$ cm and Curve *iii* at $r=10^{19}$ cm. The index of the energy spectrum at injection is $\gamma=1.52$ and the mode of energy loss synchrotron radiation throughout. The different graphs show the effect of changing the energy and position dependences of the diffusion coefficient ($D\propto E^p r^n$) and the position dependence of the energy losses ($dE/dt \propto E^2 r^m$). D is always normalised to be $7\cdot 2\,10^{26}\,\mathrm{cm^2 s^{-1}}$ at $E=6\cdot 2\,10^{11}$ eV and $r=3\cdot 10^{18}$ cm while $H_\perp=3\cdot 10^{-4}$ Gauss at $r=3\cdot 10^{18}$ cm. Because of the rapid increase of the diffusion coefficient with energy in Figs. 4 and 5, the diffusion assumption becomes invalid for $\nu>10^{16}$ Hz in these two figures (see text)

identical to Eq. (29), showing a true steady-state is achieved. On the other hand, if $(1+n)/(2-n)<0$ $(n<-1)$ we have

$$N(r,t)=\frac{n_s}{B}\frac{(n-2)}{(n+1)}(t-t_1)^{-(1+n)/(2-n)}$$

when $t-t_1$ is large and which diverges as $t-t_1\to\infty$. Thus no steady-state solution is reached. Note also that naive application of the steady-state solution $N\propto r^{-(n+1)}$ implies a divergence in N as $r\to\infty$ when $n<-1$. For these reasons, we have restricted our calculations to $-1<n<2$ in which range physically meaningful steady-state results are obtained.

3.3 Discussion of the Synchrotron Spectra for Power-law Injection

From the expressions for $N(E,r)$ for power-law injection [Eqs. (27) and (28)] we may readily calculate the synchrotron emissivity $\varepsilon(\nu,r)$ from the usual formula

$$\varepsilon(\nu,r)=(\text{constant})\int_0^\infty dEN(E,r)H_\perp(r)\frac{\nu}{\nu_c}\int_{\nu/\nu_c}^\infty K_{5/3}(\eta)d\eta\,, \tag{30}$$

where

$\nu_c=(3eH_\perp/4\pi m_0 c)\,(E/m_0c^2)^2$

(Ginzburg and Syrovatskii, Chapter 2, p. 63). When computing the synchrotron spectra from (30) we have assumed that the electron distribution is always isotropic and the direction of the magnetic field is random when averaged over unit volume. Figures 2–5 show spectra for various forms of energy loss and diffusion coefficient. Each graph is a plot of $\log\varepsilon$ vs $\log\nu$ for 3 different radii: $r=10^{18}$ cm (Curve *i*), $r=3.10^{18}$ cm (Curve *ii*) and $r=10^{19}$ cm (Curve *iii*). As the loss process of greatest interest is synchrotron, we have taken $q=2$ and $H\propto r^{m/2}$ throughout. We have also assumed $\gamma=1.52$, but the curves will be qualitatively similar for larger values of γ. In all cases, the diffusion coefficient has been scaled

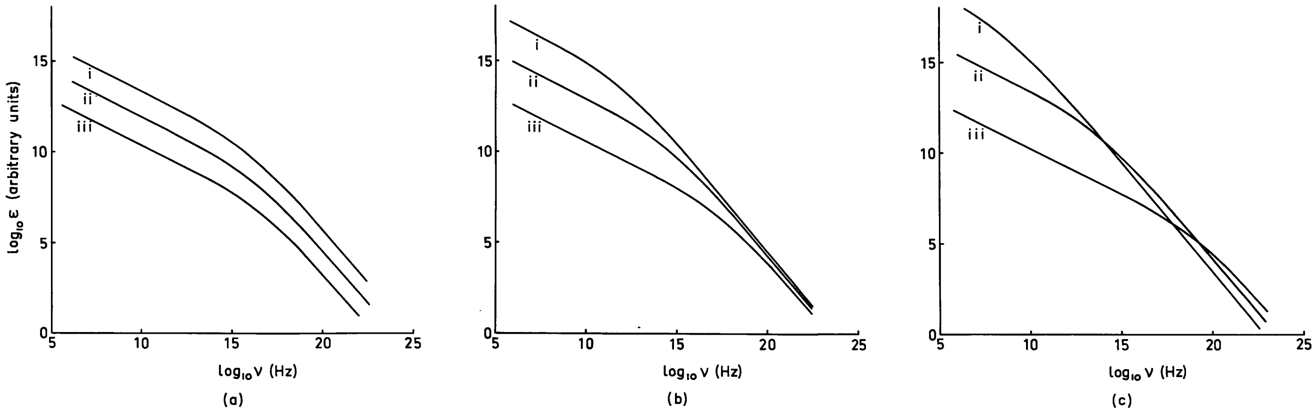

Fig. 4a—c. Illustrating the effect of changing m when $p=2$ and $n=-0.9$. (a) $m=-2$, (b) $m=0$, (c) $m=2$

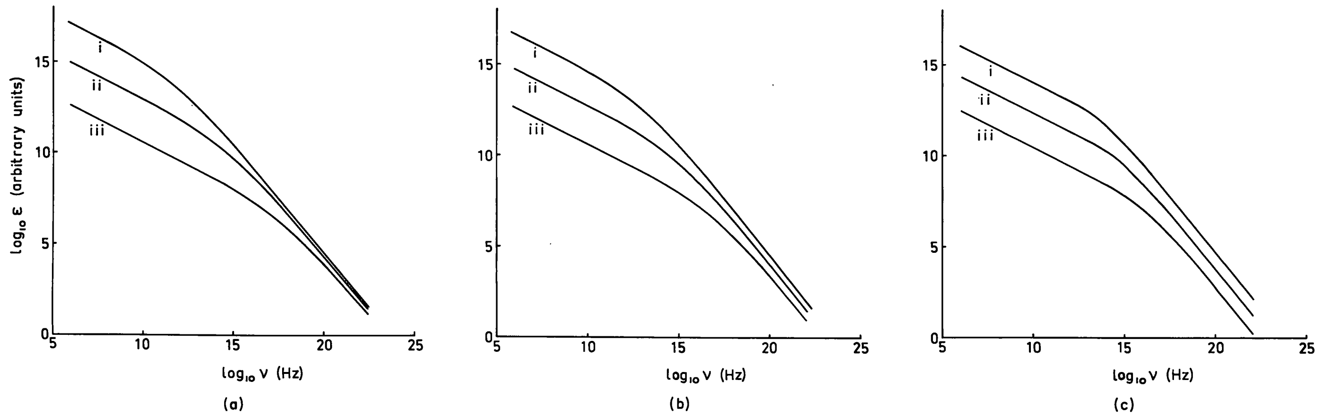

Fig. 5a—c. Illustrating the effect of changing n when $p=2$ and $m=0$. (a) $n=-0.9$, (b) $n=0$, (c) $n=0.9$

to be 7.2×10^{26} cm^2 s^{-1} at $r=3\cdot10^{18}$ cm and $E=6\cdot10^{11}$ eV and the component of magnetic field perpendicular to the line of sight $H_\perp=3\cdot10^{-4}$ Gauss at the same radius [these values are appropriate to models of the Crab Nebula, see Wilson (1972)]. In Figs. 2 and 3, models with $p=0$ (diffusion coefficient independent of energy) are illustrated, while in Figs. 4 and 5, $p=2$ (diffusion coefficient $\propto E^2$) is assumed. Figures 2 and 4 illustrate the effect of changing m (the exponent in the radial dependence of dE/dt) and Figs. 3 and 5 the effect of changing n (the exponent of radius in the expression for D). We discuss each figure in turn.

1. Figure 2. $q=2$, $p=0$, $n=-0.9$, $m=-2$ (a), $m=0$ (b), $m=2$ (c).

At low energies where losses are unimportant, $N(E,r)\propto r^{-0.1}E^{-1.52}$ [Eq. (A16)]. For $m=-2$ and $m=0$ the emissivity also decreases with increasing radius ($\varepsilon\propto NH_\perp^{(\gamma+1)/2}$) but when $m=2$ the increasing field strength to larger radii dominates the decreasing density and the emissivity increases. Since the average magnetic field between $r=0$ and $r=3\cdot10^{18}$ cm progressively decreases in the sequence $m=-2$, 0, $+2$, the frequency where the spectrum begins to steepen (ν_s) for Curves (*i*) and (*ii*) increases from Fig. 2a to 2b to 2c. Beyound $r=3\cdot10^{18}$ cm, the trend of field strengths is reversed so for Curve (*iii*) ν_s is quite similar for all 3 curves. This is because the reduced rate of energy loss in the lower field at large (small) radii tends to compensate the increased rate in the higher field at small (large) radii. These arguments explain the progressive "opening out" of the high frequency curves as one goes from Fig. 2a to 2c.

2. Figure 3. $q=2$, $p=0$, $m=0$, $n=-0.9$ (a), $n=0.0$ (b), $n=0.9$ (c).

Since the magnetic field is now constant we have, at low frequencies, $\varepsilon\propto N(E,r)\propto r^{-(n+1)}E^{-1.52}$. The differences in the high frequency spectra between the three figures may be accounted for as follows. The average diffusion coefficient between $r=0$ and $r=3\cdot10^{18}$ cm progressively decreases in the sequence $n=-0.9$, 0, $+0.9$ and so ν_s for Curves (*i*) and (*ii*) decreases as n increases (a large diffusion coefficient implies fast diffusion, so that at any given radius the electrons are predominantly young and ν_s correspondingly high). Beyond $r=3\cdot10^{18}$ cm, this trend of the diffusion coefficient is reversed and arguments analogous to those used in connection with Fig. 2 account for the progressive "closing up" of the three curves at high frequencies as one goes from Fig. 3a to 3c.

3. Figure 4. $q=2$, $p=2$, $n=-0.9$, $m=-2$ (a), $m=0$ (b), $m=2$ (c) and Fig. 5. $q=2$, $p=2$, $m=0$, $n=-0.9$ (a), $n=0$ (b), $n=0.9$ (c).

Figures 4 and 5 differ from Figs. 2 and 3 by including an energy dependent diffusion coefficient ($D\propto E^2$). The

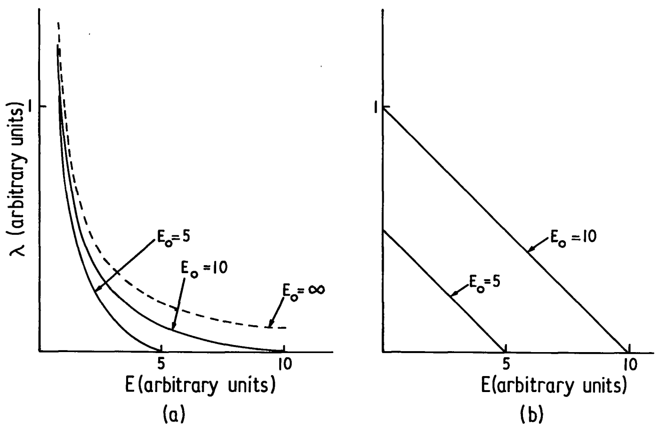

Fig. 6a and b. Plots of $\lambda=\int_{E_0}^{E}(D(E)/B(E))dE$ versus energy E. When $m=n=0$, λ represents the mean square distance from the origin of electrons (energy E), which were injected with energy E_0. (a) $p=0$, $q=2$, so $\lambda=(D_0/b)\,(1/E-1/E_0)$. Curves are given for $E_0=\infty$ (dotted) and for two other values of E_0. (b) $p=2$, $q=2$, so $\lambda=(D_0/b)\,(E_0-E)$. The two straight lines represent the behaviour for different values of E_0

most important difference which results is that it is now the *low* frequency spectra which are most affected by the synchrotron losses. Such an effect arises since, at any given radius, the high energy electrons are, on average, now much younger than low energy ones. Thus, in spite of the faster *rate* of energy loss at high energies, the low-energy electrons are affected more strongly by the losses. In these models, the size of the source *increases* with increasing frequency at low frequencies. Such an "inverted" situation will arise whenever $p>1$ (for $q=2$). When $p=1$, the faster rate of diffusion of the high energy electrons just compensates for their faster rate of energy loss and the spectra are power laws of index $\alpha=-\gamma/2$ over the whole frequency range.

The effect of variation of parameters m and n in Figs. 4 and 5 may be understood by arguments analogous to those used for Figs. 2 and 3.

Next we add a word of warning about Figs. 4 and 5. Because of the rapid increase of diffusion coefficient with energy, the corresponding mean free path (l) of the electrons ($l\sim 3D/c$) is 10^{18} cm at $E=2.5\,10^{12}$ eV. At higher energies, therefore, most electrons are not scattered before they reach the radii at which we have calculated the emissivity. Under these circumstances, the diffusion assumption is invalid (the motion corresponds more closely to free streaming), the electron density cannot be calculated using Eq. (28) and the synchrotron spectra will be incorrect for $\nu\gtrsim 10^{16}$ Hz. As Figs. 4 and 5 are intended only to give physical expression to Eq. (28) we have not corrected them for this effect.

The difference between the spectra for cases with $p-q+1<0$ on the one hand (e.g. Figs. 2 and 3) and $p-q+1>0$ on the other (e.g. Figs. 4 and 5) may be further clarified by considering the dependence of the parameter $\lambda=\int_{E_0}^{E}\frac{D(E)}{B(E)}dE$ on energy E, when the diffusion coefficient and rate of energy loss do not depend on radius ($m=n=0$). It may be easily seen that λ then represents the mean square distance from the origin of a particle with energy E, the particle having been injected with energy $E_0(E_0>E)$. Graphs of λ versus E are shown in Fig. 6. In Fig. 6a we have taken $p=0$, $q=2$ and in Fig. 6b $p=2$, $q=2$. Electrons are injected at $\lambda=0$ and $E=E_0$ and move to smaller energy and larger λ. Trajectories are shown in each graph for two different values of E_0 and, in addition, for $E_0=\infty$ in Fig. 6a. When $p=0$, $q=2$ (Fig. 6a), there are very few electrons above an energy $E=D_0/b\lambda$ (dotted curve). This sharp cut-off explains the exponential decay of the synchrotron emissivities at high frequencies in Figs. 2 and 3. However, no such sharp cut-off occurs when $p=2$, $q=2$ (Fig. 6b); for any given λ, all values of E are permitted and the synchrotron spectra (Figs. 4 and 5) are much smoother.

3.4. The Integrated Spectrum

i) Preamble

Many observations of radio sources determine only the integrated emission and not the distribution of brightness. It is, therefore, important to determine the shape of the integrated spectrum in our models. Because these apply to infinite space, we cannot, strictly speaking, take account of the source boundary correctly. However, if we envisage a spherical radio source of radius R, with the particles being generated at the centre, an approximate solution may be obtained by applying the equation inside the source and assuming no emission from outside it. In the regime where energy losses are large, the result will be an excellent approximation, since no electrons of these energies can reach the boundary, whose effects are, therefore, negligible. In the other domain, where particles can reach the boundary before losing much energy, the solution will depend on the nature of the boundary condition at $r=R$. The extreme possibilities are a perfectly absorbing and a perfectly reflecting boundary and we may expect our solution to correspond more closely to the former, since the predominant motion of the particles is, after all, towards larger radii.

The models allow for variation of energy losses with radius ($dE/dt\propto r^m$). When the losses are synchrotron, the corresponding variation of magnetic field must be taken into account when calculating the synchrotron spectra. Since this type of loss is our main interest, we give the derivation of the integrated spectrum for $H\propto r^{m/2}$ (cf. Section 3.3). Cases in which the dependence of H on r is not directly related to m (such as inverse Compton, ionisation or bremsstrahlung losses) may be dealt with by an analogous procedure.

ii) Calculation

We shall make the "monochromatic" approximation i.e. an electron of energy E radiates a power of

$$P=(2c/3)\,(e^2/m_0c^2)^2H_\perp^2(r)\,(E/m_0c^2)^2 \qquad (31)$$

at a frequency ν where

$$\nu=(0.29\times 3eH_{\perp}(r)E^2)/(4\pi m_0^3c^5)\,. \qquad (32)$$

The procedure is to calculate first the radiation emitted in a spherical shell of radius r and thickness dr, which is

$$I_\nu d\nu dr=(\text{constant})\cdot r^{2+m/4}\nu^{1/2}N(E,r)drd\nu\,.$$

From the whole source

$$I_\nu d\nu=(\text{constant})\,\nu^{1/2}d\nu\int_0^R r^{2+m/4}N(E,r)dr\,, \qquad (33)$$

where R is the radius of the source. We must now substitute for $N(E,r)$ from Eq. (27) or (28) depending on the sign of $p-q+1$.

a) $p-q+1<0$.

Substituting (27) in (33) and changing from variables E and r to ν and z where

$$z=[b(q-p-1)r^{m-n+2}]/[(m-n+2)^2D_0E^{p-q+1}]$$

one has

with

$$\alpha=\frac{(p-q+1)}{2}\cdot\left\{\frac{3-(m/4)(-\gamma-q-(p-q+1)(m+3)/(m-n+2))}{m-n+2+(m/4)(p-q+1)}\right\}$$
$$+1/2(-\gamma+2-q-(p-q+1)(m+3)/(m-n+2))\,. \qquad (37)$$

b) $p-q+1>0$.

We must now substitute Eq. (28) for $N(E,r)$, but find exactly the same frequency dependence for $I_\nu d\nu$ as the case $p-q+1<0$ [see Eqs. (36) and (37)]. When the energy losses are negligible, the condition for convergence of the integral is, again, Eq. (35). When the losses are large, however, the integration has the form

$$\int_0^\infty z^{d-1}U(a_1,c,z)dz$$
$$=(\Gamma(d)\Gamma(a_1-d)\Gamma(d-c+1))/(\Gamma(a_1)\Gamma(a_1-c+1))$$

$$I_\nu d\nu=(\text{constant})\cdot\nu^{1/2(-\gamma+2-q-(p-q+1)(m+3)/(m-n+2))}$$
$$\cdot\,\nu^{-m/4\left\{\frac{p-q+1}{2(m-n+2+(m/4)(p-q+1))}\right\}\cdot\{-\gamma-q-12/m-((p-q+1)(m+3)/(m-n+2))\}}$$
$$\cdot\int_0^{z_0}z^{\frac{3-m/4(-\gamma-q-((p-q+1)(m+3)/(m-n+2)))}{m-n+2+(m/4)(p-q+1)}-1}e^{-z}U(a_0,c,z)dz\,, \qquad (34)$$

where

$$z_0=\frac{b(q-p-1)R^{m-n+2+(m/4)(p-q+1)}\nu^{-(p-q+1)/2}}{(m-n+2)^2D_0A^{p-q+1}}\,,$$

$$a_0=(1-\gamma)/(p-q+1)\,,$$

$$c=1+(n+1)/(m-n+2)\,,$$

and A is a constant. The integral may be simply evaluated in the two extreme cases of no energy losses and strong energy losses.

Losses negligible.

This means $z\ll 1$ throughout the source so we may use the small argument expansion for U:

$$U(a_0,c,z)\sim(\Gamma(c-1)z^{1-c})/\Gamma(a_0) \qquad z\ll 1\,.$$

The resulting integral converges at its lower limit if

$$\frac{3-(m/4)(-\gamma-q-(p-q+1)(m+3)/(m-n+2))}{m-n+2+(m/4)(p-q+1)}-\frac{(n+1)}{(m-n+2)}>0 \qquad (35)$$

in which case

$$I_\nu d\nu\propto\nu^{-(\gamma-1+p)/2}d\nu \qquad (36)$$

as we would expect from the energy spectra for small losses [Eq. (A16)].

Losses large.

In this regime, few electrons reach the edge and the upper limit of the integral may be put equal to ∞. Convergence at this upper limit is assured by the exponential term and at the lower one when Eq. (35) is satisfied. We then find a power law in frequency

$$I_\nu\propto\nu^\alpha d\nu$$

if $0<\mathscr{R}d<\mathscr{R}a_1$, $\mathscr{R}c<\mathscr{R}d+1$ (38) (Erdelyi *et al.*, 1953, p. 285), where

$$d=\frac{3-(m/4)(-\gamma-q-(p-q+1)(m+3)/(m-n+2))}{m-n+2+(m/4)(p-q+1)}$$

$$a_1=((p-q+\gamma)/(p-q+1))+((n+1)/(m-n+2))$$

and c and z have the same meanings as in Eq. (34). Thus Eq. (38) become

$$\frac{p-q+\gamma}{p-q+1}+\frac{n+1}{m-n+2}$$
$$>\frac{3-(m/4)(-\gamma-q-(p-q+1)(m+3)/(m-n+2))}{m-n+2+(m/4)(p-q+1)}$$
$$>\frac{n+1}{m-n+2}$$

under which conditions we have a spectrum of the form of Eq. (37).

iii) Physical Discussion

The integral spectrum for *no energy losses* [Eq. (36)] depends only on γ, the index of the injected energy spectrum and p the exponent of energy in the diffusion coefficient (p determines the variation with energy of the leakage time from the source). For *large losses*, the spectral index is more complicated [Eq. (37)] but if the magnetic field is uniform ($m=0$) we find

$$I_\nu d\nu\propto\nu^{(-\gamma+2-q)/2}\,.$$

For the rest of this section, we take $q=2$ (appropriate to synchrotron losses) and then have

$$I_\nu\propto\nu^{-\gamma/2}\,.$$

Thus, if $p=m=0$ the spectrum shows a change of spectral index of 0.5 [from $-(\gamma-1)/2$ to $-\gamma/2$], a very well-known result. The reason for the integrated spectrum being independent of n and p in the high energy loss regime when $m=0$ is quite simple. As long as the electrons lose most of their energy inside the source, their exact spatial distribution is unimportant for the integrated spectrum. However, when the magnetic field varies with r ($m \neq 0$), the integrated spectrum also depends on m, n and p. Thus, *in models with* $m \neq 0$, *the change of spectral index between low and high frequency regimes is not, in general, equal to* 0.5. In particular, if

$$\left|\frac{4}{m}\frac{(m-n+2)}{(p-q+1)}\right| \ll 1,$$

and bearing in mind Eq. (23), eq. (37) becomes

$$\alpha \simeq -1 - \frac{(m-n+2)}{(p-q+1)}\frac{2}{m}\left[\gamma+q+\frac{12}{m}-\frac{4(m+3)}{m}\right]$$

or $\alpha \to -1$ when the second term is neglected. Such α could be achieved, for example, by taking $m \simeq -2$ (i.e. $H \propto r^{-1}$) and $n \sim 0$. It is interesting that the spectral index of the integrated X-ray emission from the Crab Nebula is -1.1 to -1.2 (Peterson and Jacobson, 1970) while at radio frequencies it is -0.26 (Baldwin, 1971). This spectrum could be explained by taking $\gamma = 1.52$ over the whole range of injected energies, $p=0$ for electrons radiating radiofrequencies, $m \sim -2$ and $n \sim 0$. The *ad hoc* postulate of a steeper injection spectrum at X-ray energies than at radio energies (Wilson, 1972; Rees and Gunn, 1974) is thereby rendered unnecessary and instead a simple power law injection spectrum from $E = 10^8$ eV to 10^{14} eV taken. We defer a more detailed comparison of our models with the observations to a later date.

Acknowledgements. I wish to thank Dr. B. J. Burn for stimulating discussions on diffusion processes and Dr. R. H. Harten for advice on computer programming. Professor F. D. Kahn and Dr. A. G. de Bruyn have made numerous helpful comments on the manuscript. I am grateful to the Royal Society for a European Program Fellowship.

Appendix

We first consider the case of a monoenergetic injection spectrum and then integrate the result to obtain the solution appropriate to a power law injection spectrum.

Monoenergetic Injection Spectrum.

The diffusion-loss equation for our situation is

$$\frac{\partial N}{\partial t} - \operatorname{div}[D(E,r)\operatorname{grad} N] + \frac{\partial}{\partial E}\left[N\frac{dE}{dt}(E,r)\right] = \delta(r)\delta(E-E_0)K(E_0). \tag{A1}$$

Except at $r=0$

$$\frac{\partial N}{\partial t} - \operatorname{div}[D(E,r)\operatorname{grad} N] + \frac{\partial}{\partial E}\left[N\frac{dE}{dt}(E,r)\right] = 0. \tag{A2}$$

We shall first solve (A2), then match the solution to appropriate boundary conditions at $r=0$ and $r=\infty$ to obtain the solution of (A1). We search for a steady-state solution, express D and dE/dt by Eqs. (19) and (20) and our differential equation becomes

$$-\frac{D(E)}{r^2}\frac{\partial}{\partial r}\left(r^{n+2}\frac{\partial N}{\partial r}\right) + r^m\frac{\partial}{\partial E}(NB(E)) = 0. \tag{A3}$$

To solve (A3) first change variables to y and λ from N and E:

$$y = N(E,r)B(E)$$

$$\lambda = \int_{E_0}^{E}\frac{D(E)}{B(E)}dE$$

and then transform the equation using the Laplace operator $\int_0^\infty \exp(-q\lambda)d\lambda$ obtaining

$$-\frac{1}{r^2}\frac{\partial}{\partial r}\left(r^{n+2}\frac{\partial\bar{y}}{\partial r}\right) + r^m(q\bar{y} - y(\lambda=0)) = 0,$$

where

$$\bar{y} = \int_0^\infty y\exp(-q\lambda)d\lambda.$$

For $r \neq 0$, $N(E_0, r) \to 0 \therefore y(\lambda=0) \to 0$.

After a further variable change to v and z:

$$v = r^{(n+1)/2}\bar{y}$$

$$z = \sqrt{q}\cdot\frac{2}{(m-n+2)}\cdot r^{(m-n+2)/2}$$

we find

$$z^2v'' + zv' - \{z^2 + ((n+1)/(m-n+2))^2\}v = 0, \tag{A4}$$

where $v' = \dfrac{\partial v}{\partial z}$.

This is the modified Bessel's equation. Solutions are

$I_{\pm(n+1)/(m-n+2)}(z)$ and $K_{(n+1)/(m-n+2)}(z)$

(e.g. Abramowitz and Stegun, 1965).

$I_{(n+1)/(m-n+2)}(z)$ and $I_{-(n+1)/(m-n+2)}(z)$

are linearly independent except when $(n+1)/(m-n+2)$ is an integer, while $I_{(n+1)/(m-n+2)}(z)$ and $K_{(n+1)/(m-n+2)}(z)$ are linearly independent for all $(n+1)/(m-n+2)$.

To simplify matters we now assume $m-n+2>0$ (A5) and $n+1>0$ (A6). To choose the appropriate solution, we appeal to boundary conditions at $r=0$ and $r=\infty$

i) As $r \to \infty$, we require $N \to 0$ implying

$$v = AK_{(n+1)/(m-n+2)}(z), \tag{A7}$$

where A is independent of z.

ii) As $r \to 0$, we assume N tends to the solution for *no* energy losses. This is because electrons at the origin have just been created there and have lost no energy. The steady-state solution for no energy losses is

$$N(E,r) = \frac{K(E_0)\delta(E-E_0)}{4\pi D(E)}\frac{r^{-(n+1)}}{(n+1)}$$

or in terms of v, q and z

$$v = \frac{K(E_0)}{4\pi(n+1)}\left[\frac{(m-n+2)}{2}\frac{1}{\sqrt{q}}\right]^{-(n+1)/(m-n+2)} \cdot z^{-(n+1)/(m-n+2)}. \tag{A8}$$

Expanding (A7) for small z and equating to (A8) we may find A and thus the final solution for v. All that remains is to convert from variables v, q and z back to N, E and r. The conversion from q to λ is effected by using the fact that the inverse Laplace Transformation of

$$2\alpha^{1/2}q^{\mu-1}K_{2\nu}(2\alpha^{1/2}q^{1/2})$$

is equal to

$$\lambda^{1/2-\mu}\exp(-\alpha/2\lambda)W_{\mu-1/2,\nu}(\alpha/\lambda),$$

where W is a Whitaker function (Erdelyi *et al.*, 1954, p. 283). Alternatively the solution may be expressed in terms of the confluent hypergeometric function of the second kind since

$$W_{\mu-1/2,\nu}(\alpha/\lambda)=\exp(-\alpha/2\lambda)(\alpha/\lambda)^{1/2+\nu}\cdot U(1+\nu-\mu,1+2\nu,\alpha/\lambda).$$

In our case

$$\nu=\frac{n+1}{2(m-n+2)},\quad \mu=1+\frac{n+1}{2(m-n+2)},$$

$$\alpha=\frac{r^{m-n+2}}{(m-n+2)^2}$$

and since $1+\nu-\mu=0$, the final solution becomes

$$N(E,r)=\frac{(m-n+2)^{-2(n+1)/(m-n+2)}}{\Gamma\left(\frac{n+1}{m-n+2}\right)4\pi(n+1)}\cdot\frac{K(E_0)}{|B(E)|}$$

$$\cdot\left[\textstyle\int_{E_0}^{E}D(E)/B(E)dE\right]^{-(m+3)/(m-n+2)} \quad \text{(A9)}$$

$$\cdot\exp\left\{-\frac{r^{m-n+2}}{(m-n+2)^2\int_{E_0}^{E}D(E)/B(E)dE}\right\}.$$

Putting $m=n=0$ in Eq. (A9) yields

$$N(E,r)=\frac{K(E_0)}{\{4\pi\int_{E_0}^{E}D(E)/B(E)dE\}^{3/2}}\frac{1}{|B(E)|}\cdot\exp\left\{-\frac{r^2}{4\int_{E_0}^{E}D(E)/B(E)dE}\right\} \quad \text{(A10)}$$

which has been found by Syrovatskii (1959).

Power-law Injection Spectrum

We now take $K(E_0)=KE_0^{-\gamma}$ $\quad E_1<E_0<E_*$

$=0 \quad E_0<E_1$ or $E_0>E_*$.

The solution for the electron density is, from (A9):

$$N(E,r)=\frac{(m-n+2)^{-2(n+1)/(m-n+2)}}{\Gamma\left(\frac{n+1}{m-n+2}\right)4\pi(n+1)}\cdot\frac{1}{|B(E)|}$$

$$\cdot\int_{E_0^{\min}}^{E_0^{\max}}KE_0^{-\gamma}\left[\textstyle\int_{E_0}^{E}D(E)/B(E)dE\right]^{-(m+3)/(m-n+2)} \quad \text{(A11)}$$

$$\cdot\exp\left\{-\frac{r^{m-n+2}}{(m-n+2)^2\int_{E_\eta}^{E}D(E)/B(E)dE}\right\}\cdot dE_0.$$

If $E<E_1$, $E_0^{\min}=E_1$ but if $E>E_1$, $E_0^{\min}=E$. For $E>E_*$, $N(E,r)=0$ and when $E<E_*$ we must put $E_0^{\max}=E_*$. Let us now substitute

$$D(E)=D_0E^p, \quad \text{(A12)}$$

and

$$B(E)=-bE^q, \quad \text{(A13)}$$

where b is a positive number, in Eq. (A11). We assume $E>E_1$ and take $E_0^{\max}=\infty$.

Thus:

$$N(E,r)=\frac{(m-n+2)^{-2(n+1)/(m-n+2)}}{\Gamma\left(\frac{n+1}{m-n+2}\right)4\pi(n+1)}\frac{K}{bE^q}$$

$$\cdot\left[\frac{b(q-p-1)}{D_0}\right]^{(m+3)/(m-n+2)}$$

$$\cdot E^{-\frac{(p-q+1)(m+3)}{(m-n+2)}}\int_E^\infty E_0^{-\gamma}\left\{1-\left(\frac{E_0}{E}\right)^{p-q+1}\right\}^{-(m+3)/(m-n+2)}$$

$$\cdot\exp\left\{-\frac{b(q-p-1)r^{m-n+2}}{(m-n+2)^2D_0E^{p-q+1}[1-(E_0/E)^{p-q+1}]}\right\}dE_0.$$

By changing the integration variable, we may obtain a form related to the confluent hypergeometric function of the second kind. The substitution necessary depends on the sign of $p-q+1$.

i) $p-q+1<0$.

Let $t=\left\{1-\left(\frac{E_0}{E}\right)^{p-q+1}\right\}^{-1}$

whence the integral becomes

$$\int_1^\infty(t-1)^{\frac{1-\gamma}{p-q+1}-1}t^{\frac{\gamma-1}{p-q+1}+\frac{n+1}{m-n+2}}$$

$$\cdot\exp\left\{-\frac{b(q-p-1)r^{m-n+2}t}{(m-n+2)^2D_0E^{p-q+1}}\right\}dt. \quad \text{(A14)}$$

Now

$$\Gamma(a)U(a,c,z)=e^z\int_1^\infty e^{-zt}(t-1)^{a-1}t^{c-a-1}dt$$

for $\mathscr{R}a>0$ and $\mathscr{R}z>0$ (Abramowitz and Stegun, 1965, p. 505).

Thus the solution for $N(E,r)$ is

$$N(E,r)=\frac{(m-n+2)^{-2(n+1)/(m-n+2)}K\Gamma\left(\frac{1-\gamma}{p-q+1}\right)}{4\pi(n+1)\Gamma\left(\frac{n+1}{m-n+2}\right)b(q-p-1)}$$

$$\cdot\left[\frac{b(q-p-1)}{D_0}\right]^{(m+3)/(m-n+2)}$$

$$\cdot E^{-\gamma+1-q-\frac{(p-q+1)(m+3)}{(m-n+2)}}$$

$$\cdot\exp\left\{-\frac{b(q-p-1)r^{m-n+2}}{(m-n+2)^2D_0E^{p-q+1}}\right\}$$

$$\cdot U\left(\frac{1-\gamma}{p-q+1},1+\frac{n+1}{m-n+2},\frac{b(q-p-1)r^{m-n+2}}{(m-n+2)^2D_0E^{p-q+1}}\right) \quad \text{(A15)}$$

as long as $n+1>0$

$m-n+2>0$

and $\gamma>1$.

Putting $m=n=p=0$, Eq. (A15) reduces to Eq. (14).

Of interest are the forms of Eq. (A15) for small and large energy losses. In the former case

$$\frac{b(q-p-1)r^{m-n+2}}{(m-n+2)^2 D_0 E^{p-q+1}} \ll 1$$

and we have

$$N(E,r)=\frac{KE^{-\gamma}}{4\pi(n+1)D_0 E^p r^{n+1}} \tag{A16}$$

as expected. For large energy losses

$$\frac{b(q-p-1)r^{m-n+2}}{(m-n+2)^2 D_0 E^{p-q+1}} \gg 1$$

one finds:

$$N(E,r)=(m-n+2)^{-2\left[\frac{n+1}{m-n+2}+\frac{\gamma-1}{p-q+1}\right]}$$

$$\cdot\left|\frac{b(q-p-1)}{D_0}\right|^{\frac{n+1}{m-n+2}+\frac{\gamma-1}{p-q+1}}$$

$$\cdot\frac{K\Gamma\left(\frac{1-\gamma}{p-q+1}\right)}{4\pi D_0(n+1)\Gamma\left(\frac{n+1}{m-n+2}\right)}$$

$$\cdot E^{-2\gamma+2-q-\frac{(p-q+1)(m+3)}{(m-n+2)}}$$

$$\cdot r^{\frac{(m-n+2)(\gamma-1)}{(p-q+1)}}\cdot\exp\left\{-\frac{b(q-p-1)r^{m-n+2}}{(m-n+2)^2 D_0 E^{p-q+1}}\right\}. \tag{A17}$$

(ii) $p-q+1>0$.

For this case we substitute

$$t=1-\{1-(E_0/E)^{p-q+1}\}^{-1}$$

and an integral of similar form to Eq. (A14) results. The solution for the electron density is then

$$N(E,r)$$

$$=\frac{(m-n+2)^{-2(n+1)/(m-n+2)}K\Gamma\left(\frac{p-q+\gamma}{p-q+1}+\frac{n+1}{m-n+2}\right)}{4\pi(n+1)\Gamma\left(\frac{n+1}{m-n+2}\right)b(p-q+1)}$$

$$\cdot\left|\frac{b(p-q+1)}{D_0}\right|^{(m+3)/(m-n+2)}$$

$$\cdot E^{-\gamma+1-q-\frac{(p-q+1)(m+3)}{(m-n+2)}}$$

$$\cdot U\left(\frac{p-q+\gamma}{p-q+1}+\frac{n+1}{m-n+2},1+\frac{n+1}{m-n+2},\frac{b(p-q+1)r^{m-n+2}}{(m-n+2)^2 D_0 E^{p-q+1}}\right) \tag{A18}$$

as long as:

$n+1>0$

$m-n+2>0$

$\gamma>1$.

For small energy losses Eq. (A18) becomes Eq. (A16) while when the losses are large the electron density is

$$N(E,r)=\frac{(m-n+2)^{2\left(\frac{p-q+\gamma}{p-q+1}\right)}K\Gamma\left(\frac{p-q+\gamma}{p-q+1}+\frac{n+1}{m-n+2}\right)}{4\pi(n+1)\Gamma\left(\frac{n+1}{m-n+2}\right)D_0}$$

$$\cdot\left[\frac{b(p-q+1)}{D_0}\right]^{-\left(\frac{p-q+\gamma}{p-q+1}\right)} r^{-(n+1)-\frac{(m-n+2)(p-q+\gamma)}{(p-q+1)}} E^{-q}. \tag{A19}$$

It is interesting that Eq. (A19) shows a power-law in energy, of slope $=-q$, i.e. the shape of the spectrum when the losses are large is governed by the nature of the energy losses and not the original injected spectrum.

References

Abramowitz, M., Stegun, I. A. 1965, Handbook of Mathematical Functions, Dover Publications Inc.

Baldwin, J. E. 1971, in *The Crab Nebula*, I.A.U. Symposium No. 46, Eds. Davies, R. D. and Smith, F. G., p. 22, D. Reidel Co., Dordrecht, Holland

Erdelyi, A., Magnus, W., Oberhettinger, F., Tricomi, F. G. 1953, Higher Transcendental Functions Vol. I, Bateman Manuscript Project, McGraw-Hill Book Co. Inc.

Erdelyi, A., Magnus, W., Oberhettinger, F., Tricomi, F. G. 1954, Tables of Integral Transforms Vol. I, Bateman Manuscript Project, McGraw-Hill Book Co. Inc.

Ginzburg, V. L., Syrovatskii, S. I. 1964, The Origin of Cosmic Rays, Pergamon Press Ltd., Oxford

Gratton, L. 1972, *Astrophys. Space Sci.* **16**, 81

Morse, P. M., Feshbach, H. 1953, Methods of Theoretical Physics, McGraw-Hill Book Co. Inc.

Peterson, L. E., Jacobson, A. S. 1970, *Publ. Astron. Soc. Pacific* **82**, 412

Rees, M. J., Gunn, J. E. 1974, *Monthly Notices Roy. Astron. Soc.* **167**, 1

Syrovatskii, S. I. 1959, *Soviet. Astron. (A. J.)* **3**, 22

Webster, A. S. 1970, *Astrophys. Letters* **5**, 189

Webster, A. S., Longair, M. S. 1971, *Monthly Notices Roy. Astron. Soc.* **151**, 261

Wilson, A. S. 1972, *Monthly Notices Roy. Astron. Soc.* **160**, 355

A. S. Wilson
Astronomy Centre, Physics Building
University of Sussex
Falmer, Brighton BN1 9QH, England